Catalysis Today 147S (2009) S336–S341

Contents lists available at ScienceDirect

Catalysis Today

journal homepage: www.elsevier.com/locate/cattod

Synergistic and size effects in selective hydrogenation of alkynes on gold nanocomposites

S.A. Nikolaev *, V.V. Smirnov

Department of Chemistry, M.V. Lomonosov Moscow State University, 1 Leninskie Gory, 119991 Moscow, Russian Federation

ARTICLE INFO

Article history:
Available online 31 July 2009

Keywords:
Heterogeneous catalysis
Au/Al_2O_3
$Au-Ni/Al_2O_3$
Synergism
Size effect
Hydrogenation
Acetylene
Phenylacetylene

ABSTRACT

Au/Al_2O_3 nanocomposites possess high activity and stability in the selective hydrogenation of phenylacetylene at 423 K. Strong dependences of the activity and selectivity on the particle size were revealed: as the diameter of gold nanoparticles was decreased from 30 to 2.5 nm, the TOF of phenylacetylene hydrogenation increased from 0.028 to 0.142 s^{-1} and the selectivity of styrene formation increased by an order of magnitude. The same trends were observed in the hydrogenation of acetylene into ethylene on supported gold. The nature of the obtained dependences is discussed in terms of "Geometric" and "Electronic" size effects.

A synergistic catalytic effect was revealed for $Au-Ni/Al_2O_3$: the conversion of acetylene on the Au-Ni catalysts was higher than the sum of conversions on Au and Ni catalysts by an order of magnitude. The appearance of synergistic activity in $Au-Ni/Al_2O_3$ is discussed in terms of formation of new $A^{\sigma+}$ catalytic sites with improved adsorption and catalytic properties due to electron transfer from gold to oxidized nickel.

1. Introduction

Styrene and ethylene feedstock usually contain small quantities (<2%) of acetylene compounds, which poison olefin polymerization catalysts. Thus, preliminary removal of these alkynes via hydrogenation is necessary [1–3]. Usually the selective Pd-Ag catalysts are employed for this process [3]. However, their activity and stability are not good enough; hence, searching for more effective catalysts is still a topical task.

Recent studies demonstrate that nano-sized gold can catalyze hydrogenation of 1,3-butadiene, acetylene, pent-1-ene, cyclohexane, unsaturated aldehydes and prop-1-yne [4–9]. But selective hydrogenation of alkynes on Au catalysts is still poorly studied [5]. It is also known that Au-Ni catalysts possess synergistic activity in allylic isomerization of octene-1, dodecene-1 and allylbenzene [10,11]; moreover, Au-Ni catalysts were found to be less prone to deactivation [12]. Thus, application of supported monometallic gold and bimetallic Au-Ni system to selective hydrogenation of alkynes from alkyne–olefin mixtures seems to be promising from both scientific and industrial standpoints.

2. Experimental

Gold and nickel catalysts were prepared via a deposition-precipitation and a pore volume impregnation technique as described previously [11]. Gold-nickel catalysts were prepared via a combination of the deposition-precipitation and impregnation techniques as described previously [11]. Alumina γ-Al_2O_3 (IKT-02-6 M from JSC "Katalizator", Novosibirsk, S = 138 m^2/g) and α-Al_2O_3 (KN-08 from JSC "Katalizator", Novosibirsk, S = 0.6 m^2/g) were used as supports for the nanoparticles. The dispersion of the gold particles was examined by the TEM observation performed with a LEO912 AB OMEGA electron microscope with 0.1 nm resolution. For each catalyst, 300 particles of the supported catalyst were processed to determine the particle size distribution and mean particle diameters. Hydrogenation of acetylene–ethylene mixtures was carried out using a fixed-bed flow reactor. A catalyst or support (1 g) was placed in a quartz tube, heated to reaction temperature (293–423 K) for 15 min in a stream of hydrogen at a flow rate of 30 h^{-1}. The reactant gas mixture containing acetylene, hydrogen and ethylene in an 1:2:20 ratio was passed through the catalyst bed at a flow rate of 720 h^{-1}. The reactor effluents were analyzed with Tcvet-800 gas chromatograph equipped with a flame ionization detector and a 30-m PoropakT capillary column. Hydrogenation of phenylacetylene–styrene mixtures was carried out using a fixed-bed flow reactor. A catalyst or support (1 g) was placed in a quartz tube, heated to reaction temperature (318–423 K) for 15 min in a stream of hydrogen at a flow rate of

* Corresponding author. Tel.: +7 495 939 3498.
E-mail address: serge2000@rambler.ru (S.A. Nikolaev).

0920-5861/$ – see front matter © 2009 Elsevier B.V. All rights reserved.
doi:10.1016/j.cattod.2009.07.032

Table 1
Results of catalytic hydrogenation of acetylene–ethylene mixtures at 293–397 K on Au/γ-Al_2O_3, Ni/γ-Al_2O_3 and Au-Ni/γ-Al_2O_3 catalysts[a].

Run	[Au], wt.%	[Ni], wt.%	d(Au), nm	d(Ni), nm	T, K	τ, min	$\Delta(C_2H_2)$, %	$\Delta(C_2H_2)_{Au\text{-}Ni}$-$\Delta(C_2H_2)_{Au}$-$\Delta(C_2H_2)_{Ni}$, %
1	0.27	–	4.0[b]	–	357	15–480	0	–
					373		0.1	–
					390		0.3	–
2	0.02	–	2.5[c]	–	333	15–480	0	–
					377		0.1	–
					390		0.1	–
3	–	0.002		22 ± 5	293	15–480	2	–
					338		10	–
					373		22	–
					390		45	–
4	–	0.02		25 ± 6	293	15–480	5	–
					338		13	–
					373		29	–
					390		51	–
5	–	0.09		30 ± 4	293	15–480	7	–
					338		18	–
					373		40	–
					390		63	–
6	0.27	0.09	4.0	30 ± 8	293	15–720	80	73
					357		99.9	82
					373		99.9	60
					390		99.9	36
7[d]	0.27	0.09	4.0	30 ± 4	293	15–480	6	−1
					357		18	−0.1
					373		40	−0.1
					390		62	−1.2
8	0.02	0.002	2.5	25 ± 10	293	15–480	31	29
					338		80	70
					373		90	68
					390		95	49
9	0.02	0.006	2.5	25 ± 10	293	15–480	69	65
					357		90	78
					373		99.9	74
					390		99.9	51
10	0.02	0.02	2.5	25 ± 10	293	15–480	36	31
					333		60	47
					377		90	61
					390		96	44

[a] Run is the experiment number, [Au] is the weight percent of gold, [Ni] is the weight percent of nickel, d(Au) is the mean particle diameter of gold in the catalyst, d(Ni) is the mean particle diameter of nickel in the catalyst, T is the reaction temperature, τ is the time on stream, $\Delta(C_2H_2)$ is the conversion of acetylene. $\Delta(C_2H_2)_{Au\text{-}Ni}$-$\Delta(C_2H_2)_{Au}$-$\Delta(C_2H_2)_{Ni}$ is the value of synergistic effect. In every run the selectivity to ethylene formation equals 100%.
[b] The calculated TOF for Au/γ-Al_2O_3 with 4 nm gold particles is $(8–24) \times 10^{-5}$ s^{-1}.
[c] The calculated TOF for Au/γ-Al_2O_3 with 2.5 nm gold particles is 64×10^{-5} s^{-1}.
[d] Mechanical mixture of Au/γ-Al_2O_3 (Au = 0.27 wt.%) and Ni/γ-Al_2O_3 (Ni = 0.09 wt.%).

1.25–1.29 cm^3/min. The reactant gas mixture containing phenylacetylene (10–30 molar percent) and styrene (70–90 molar percent) was passed through the catalyst bed at a flow rate of 200–230 h^{-1}. The reactor effluents were analyzed with a Kristall-Lux-4000 gas chromatograph equipped with a flame ionization detector and a 50-m Thermon capillary column. The turnover frequency (TOF) for Au/Al_2O_3 was calculated as $TOF = A \times B^{-1} \times t^{-1}$ as described previously [13–15]. Here (A) is the total moles of phenylacetylene converted per total gold surface area (B) per reaction time (t). (B) was calculated as $B = B_{total} \times D$, where (B_{total}) is the total amount of gold in the catalyst sample and (D) is the degree of dispersion (i.e., the surface-to-volume ratio) for gold nanoparticles with different mean diameters d(Au) calculated in [14,15].

3. Results and discussion

3.1. TEM measurements of Au, Ni and Au-Ni nanocomposites

Au/γ-Al_2O_3 and Au/α-Al_2O_3 with gold concentrations of 0.018–2.5 wt.%, Ni/γ-Al_2O_3 with nickel concentrations of 0.002–0.09 wt.% and Au-Ni/γ-Al_2O_3 with metal concentration of 0.02–0.036 wt.% were obtained and characterized by TEM. The calculated mean diameters of the supported particles d(M) are summarized in Tables 1 and 2.

The gold size distribution in each Au/γ-Al_2O_3 sample was sharp and monomodal. Mean diameters of gold particles calculated from the maxima of the size distribution of Au/γ-Al_2O_3 catalysts with 1.8, 0.37 and 0.02 wt.% gold contents were 8, 4 and 2.5 nm, respectively (Tables 1 and 2, runs 2, 13, 15). It was found that the nanoparticles in Au/α-Al_2O_3 were larger than those in Au/γ-Al_2O_3 at approximately the same gold content (Table 2, compare runs 12, 17). This can be attributed to the much smaller surface area of α-Al_2O_3 compared to γ-Al_2O_3, which led to more effective aggregation of gold in the calcination stage [4,10].

The size distribution in Ni/γ-Al_2O_3 samples was broad and monomodal. The mean diameters of Ni particles in Ni/γ-Al_2O_3 catalysts containing 0.002, 0.02 and 0.09 wt.% of nickel were 22 ± 5, 25 ± 6 and 30 ± 4 nm, respectively (Table 1, runs 3–5). The formation of the larger particles in Ni/γ-Al_2O_3 in comparison with Au could be explained by different ways of sample preparation: it is

Table 2
Results of catalytic hydrogenation of phenylacetylene–styrene mixtures at 423 K on Au/γ-Al_2O_3 and Au/α-Al_2O_3 catalysts.

Run	[Au], %	d(Au), nm	τ, min	Molar concentration, %			$\Delta(C_8H_6)$	$S(C_8H_8)$	TOF × 10^{-5} s^{-1}
				xC_8H_6	xC_8H_8	xC_8H_{10}			
Au/γ-Al_2O_3									
11	0.018	2.5	0	9.8	90.2	0			
			60	0.01	96.7	3.29	99.9	27.33	–
			120	0.01	96.6	3.39	99.9	26.59	–
			480	0.01	96.7	3.29	99.9	27.33	–
12	0.018	2.5	0	30.2	69.8	0			
			60	16.2	80	3.8	46.36	8.50	14552
			120	16.4	79.6	4	45.36	7.97	14344
			480	16.5	79.2	4.3	45.36	7.35	14241
13	0.37	4.0	0	10.2	89.8	0			
			30	0.01	95.1	4.89	99.9	18.31	–
			120	0.01	95.0	4.99	99.9	17.96	–
			480	0.01	92.0	7.99	99.9	11.18	–
14	0.37	4.0	0	29.5	70.5	0			
			480	0.01	88.0	11.99	99.9	5.85	
15	1.8	8.0	0	9.6	90.4	0			
			30	0.01	79.4	20.59	99.9	4.31	–
			120	0.01	76.0	23.99	99.9	3.76	–
			480	0.01	70.0	29.99	99.9	3.01	–
16	1.8	8.0	0	32.0	68.0	0	–	–	–
			480	0.01	45.09	54.9	99.9	1.32	–
Au/α-Al_2O_3									
17	0.03	4.5	0	10.1	89.9	0			–
			60	0.1	95.11	4.79	99.1	18.51	–
			480	0.05	95.46	4.49	99.5	19.93	–
18	0.03	4.5	0	29	71	0			–
			60	18	76.7	5.3	37.93	5.09	13067
			480	17.6	77.6	4.8	39.31	5.82	13543
19	0.8	21	0	28.1	71.9	0			
			60	13.9	59.3	26.8	50.53	1.35	5535
			480	12.5	60.4	27.1	55.52	1.45	6142
20	2.5	30	0	30.4	69.6	0			
			60	20.8	50.4	28.8	31.58	0.73	2521
			480	20	50	30	34.21	0.77	2868

Run is the experiment number, [Au] is the weight percent of gold, d(Au) is the mean particle diameter of gold in the catalyst, τ is the time on stream, TOF is the turnover frequency. $\Delta(C_8H_6)$ was calculated as $\Delta(C_8H_6) = [\chi_0(C_8H_6)\text{-}\chi_i(C_8H_6)] \times [\chi_0(C_8H_6)]^{-1} \times 100\%$, where $\chi_0(C_8H_6)$ is the molar concentration of phenylacetylene in the initial gas mixture, $\chi_i(C_8H_6)$ is the molar concentration of phenylacetylene in the products after reaction time (i). The selectivity of the styrene formation was determined as $S(C_8H_8) = [(\chi_0(C_8H_6)\text{-}\chi_i(C_8H_6)] \times [\chi_0(C_8H_8)] \times [\chi_0(C_8H_6)]^{-1} \times [\chi_i(C_8H_{10})]^{-1}$, where $\chi_0(C_8H_6)$ and $\chi_0(C_8H_8)$ are the molar concentrations of phenylacetylene and styrene in the initial gas mixture, respectively; $\chi_i(C_8H_6)$ and $\chi_i(C_8H_{10})$ are the molar concentrations of phenylacetylene and ethylbenzene in the products after reaction time (i), respectively.

known that at the same metal loadings, impregnation catalysts contain larger particles than those obtained via deposition-precipitation [4].

The size distributions of Au-Ni catalysts were bimodal with two maxima, a sharp maximum near 2.5–4 nm and a broad one near 20–30 nm. At the first approximation, these maxima could be attributed to gold (compare mean diameters in Table 1, runs 1, 6) and nickel (compare mean diameters in Table 1, runs 5, 6); hence, Au-Ni nanocomposites could be described as a mix of supported gold and nickel nanoparticles. On the one hand, the formation of new phases (mixed bimetallic particles or intermetallics) during covering of gold particles by nickel under our synthetic conditions (see Section 2 and [11]) seems to be unlikely [12] but on the other hand, this cannot be ruled out completely.

3.2. Synergism of Au-Ni nanocomposites in selective hydrogenation of acetylene compounds

The results of acetylene–ethylene mixture hydrogenation are presented in Table 1. As expected, catalysts based on pure nickel showed better activity than those based on gold (Table 1, runs 2, 4). At a mild temperature, the selectivity to ethylene and durability of Ni/γ-Al_2O_3 were also high. However, at best, the conversion of acetylene on Ni/γ-Al_2O_3 did not exceed 63% (Table 1, run 5). These data are in good agreement with the results reviewed previously [1,3].

The gold nanoparticles supported on alumina did not catalyze any chemical transformation of acetylene or ethylene at 293–360 K (Table 1, runs 1, 2). As the temperature increased from 360 to 390 K, a low (0.1–0.3%) conversion of acetylene on gold with 100% selectivity to ethylene was detected. The durability of Au/γ-Al_2O_3 in acetylene hydrogenation at 360–390 K (Table 1, runs 1, 2) was high: no decrease in conversion occurred during 8 h. The obtained results are in a good agreement with the earlier results obtained by Jia et al. [7]. An increase in the TOF from (8–24) × 10^{-5} s^{-1} to 64 × 10^{-5} s^{-1} upon a decrease in the gold particle size from 4 to 2.5 nm was also found (Table 1, runs 1, 2). The increase in the TOF in the hydrogenation of unsaturated compounds on gold was mentioned repeatedly [4–6,16] and it seems that this trend does not depend on the nature of the unsaturated substrate, the method of catalyst preparation or temperature [4,5]. We will discuss the nature of this phenomenon in the next chapter and now just mention that the hydrogenation of acetylene was not an exception to the common rule.

The partial covering of gold nanoparticles by nickel led to a synergistic activity: the conversion of acetylene on Au-Ni nanocomposites was always higher than the sum of conversions on Au and Ni (Table 1). For example, the synergistic gain of Au-Ni/γ-Al_2O_3 (Au = 0.27%, Ni = 0.09%) at 293 K was equal to 73%, the selectivity of Au-Ni catalyst still remained 100% and the time of stable operation was at least 12 h. A decrease in the total metal loading did not affect the selectivity and stability of Au-Ni systems at 293 K but led to a decrease in the acetylene conversion (Table 1 compare runs 6, 9), though the synergistic effect was still detectable.

Our previous investigations of Au/γ-Al_2O_3 and Au-Ni/Al_2O_3 by XPS, DRIFT, and XAS techniques showed that nickel in both bimetallic Au–Ni/γ-Al_2O_3 and monometallic Ni/Al_2O_3 catalysts exists as Ni^{2+}, gold in the monometallic Au/γ-Al_2O_3 catalyst exists as Au^0 nanoclusters, whereas the Au^0 nanoclusters co-exist with Au^{3+} cations in the bimetallic Au–Ni/γ-Al_2O_3 samples [11]. Then the most probable mechanism of the Au–Ni synergism represents the electron transfer from the electron-rich Au^0 particles to the electron-deficient Ni^{2+} moieties to give new positively charged gold catalytic sites. Let us discuss the difference between these new catalytic sites and non-charged gold nanoparticles from the standpoint of selective hydrogenation of acetylene. Two main factors should be taken into account: (1) adsorption of organic substrates and (2) the change in the metal oxidation state:

(1) Acetylene and ethylene are Lewis bases sensitive to electron acceptors. An increase in the surface positive charge on Au due to electron transfer [11] improves the electron acceptor properties of gold and thereby should lead to stronger adsorption of acetylene or ethylene on $Au^{\delta+}$ than on Au^0 and, therefore, increase the probability of the chemical reaction;
(2) Catalytic hydrogenation of acetylene can be described by Scheme 1 [3].

The main feature of this scheme is the catalytic oxidation–reduction cycle $M^n \rightarrow M^{n+2} \rightarrow M^n$. In the case of non-charged zero-valence gold nanoparticles, this cycle should look like $(Au_{n+1})^0 \rightarrow (Au_n)Au^{+2} \rightarrow (Au_{n+1})^0$. But these valence changes seem to be improbable for gold, as the typical gold oxidation states are 0, +1, and +3 rather than +2. However, if supported gold nanoparticles may carry a positive charge +3 or +1, then a highly probable catalytic cycle with common gold valence changes will be obtained: $(Au_n)Au^{+1} \rightarrow (Au_n)Au^{+3} \rightarrow (Au_n)Au^{+1}$.

Good evidence for the proposed mechanism could be provided by the found dependence of the synergistic effect on the [Au]/[Au+Ni] molar ratio (Fig. 1). The last left point in Fig. 1 corresponds to Au/Al_2O_3 ([Au]/[Au+Ni] of 100%) with supported Au^0 particles and zero activity. The covering of the gold nanoparticles by nickel led to formation of positively charged Au. This should result in a higher conversion (see Fig. 1, as [Au]/[Au + Ni] decreased from 100% to 50%, the conversion increased). Certainly, further covering of gold nanoparticles by nickel (see Fig. 1, [Au]/[Au + Ni] of 1–50%) also gave rise to positively charged gold. But at the same time, the concentration of supported nickel became substantial and nickel particles started to partially block the access of reaction substrates to the gold sites (see Fig. 1, as [Au]/[Au + Ni] decreased from 50% to

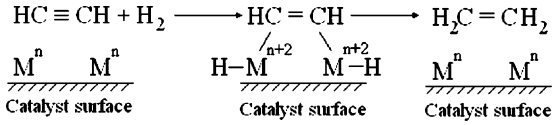

Scheme 1. Hydrogenation of acetylene on the surface of heterogeneous catalysts [3].

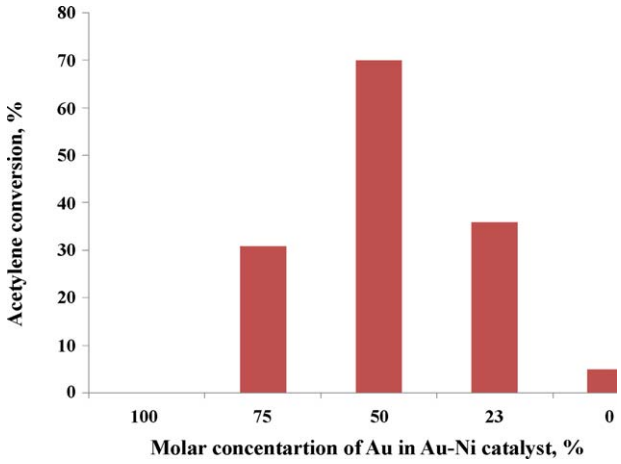

Fig. 1. Acetylene conversion vs. the molar ratio [Au]/[Au] + [Ni] in Au-Ni/γ-Al_2O_3 catalysts. Reaction conditions: T = 293 K, [Au] + [Ni] = 0.02–0.04 wt.%.

1%, the conversion decreased). Finally, in the last right point in Fig. 1, supported Ni nanoparticles cause only 5% conversion of acetylene.

One more piece of evidence for the proposed mechanism is provided by the dependence of synergistic effect on the reaction temperature. The increase in the reaction temperature from 293 to 350 K led to an increase in the synergistic gain, but further increase in the reaction temperature caused the opposite effect (Table 1 runs 6, 8–10). The same situation was observed in the hydrogenation of phenylacetylene at 423 K, in particular, at this temperature, Au-Ni catalysts did not posses any synergistic properties. The positive influence of the temperature rise from 293 to 350 K on the hydrogenation is usual and is attributable to an increase in the rate of dissociative adsorption of hydrogen [1,3,8]. The nature of the negative influence should be examined more thoroughly. It is important to mention that in the absence of close contact between gold and nickel, no synergistic effect occurs (Table 1, compare runs 7, 6). Thus, the detected decrease in the synergistic effect of Au-Ni catalysts with increase in the reaction temperature from 350 K could be explained by increase in the supported cluster mobility [4], resulting in the loss of close contact between the gold and nickel particles. This certainly leads to a decrease in the $Au^{\delta+}$ concentration and lowering of the hydrogenation rate. Moreover, high temperature favored the complete reduction of Ni^{2+} in Au-Ni samples. Thus the formation of new $Au^{\delta+}$ via electron transfer from the electron-rich Au^0 particles to the electron-deficient Ni^{2+} is also suppressed.

3.3. The dependences of activity and selectivity on the size of supported gold nanoparticles in the selective hydrogenation of acetylene compounds

The experimental data of hydrogenation of the phenylacetylene–styrene mixtures on Au/γ-Al_2O_3 and Au/α-Al_2O_3 are summarized in Table 2. No significant difference was observed between catalytic hydrogenation on the same-size nanopartilces supported on γ-Al_2O_3 or α-Al_2O_3: the conversion, the selectivity and the catalyst durability were approximately equal (Table 2, compare runs 13, 17). Thus, the type of alumina does not have significant influence on the catalytic properties of supported gold in this reaction.

Depending on the phenylacetylene concentration, its conversion on the supported gold nanoparticles varied from 30 to 99.99%. During each run (Table 2, runs 11–20), the conversion was constant for at least 4 h. The observed conversion values and excellent durability were in agreement with data of the present paper (see

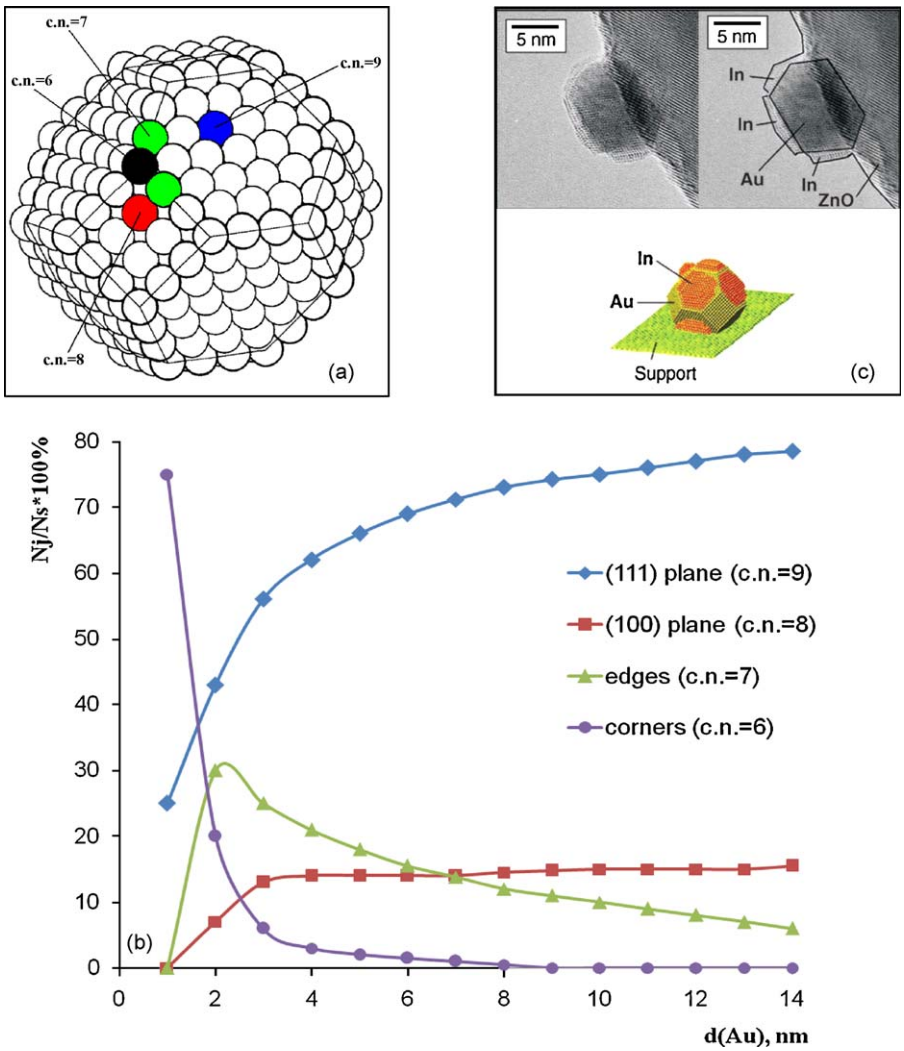

Fig. 2. Cuboctahedron model of gold nanoparticle (a) and dependence of relative numbers of surface sites N_j/N_s on the diameters of cuboctahedron gold particles (b), where N_j is the number of surface atoms with coordination number j, N_s is the total number of surface atoms (as given in [16]). HRTEM image of real Au-In/ZnO catalyst (c). Indium preferentially decorates the outer faces of the gold particles while the edges remain uncovered (as given in [15]).

Table 1, runs 1–2 at 390 K) and the earlier published works [6,7,17]).

The TOF calculated at approximately equal (30–50%) conversions on 2.5, 4.5, 20 and 30 nm gold nanoparticles at 423 K were 0.142, 0.135, 0.061 and 0.028 s^{-1} respectively (Table 2, runs 12, 18–20). These data, on the whole, are also comparable with both the TOF in hydrogenation of acetylene on gold (Table 1, runs 1, 2 T = 360–390 K) and the TOF on the same-size gold particles supported on Al_2O_3 in hydrogenation of unsaturated compounds [13,9]. The TOF in the phenylacetylene and acetylene hydrogenation was correlated with the particle size (Table 1, runs 1, 2 T = 370–390 K and Table 2, runs 12, 18–20). The size dependence of the selectivity was also detected: as the size of gold nanoparticles was decreased from 30 to 2.5 nm, the selectivity of styrene formation (S) increased by an order of magnitude (Table 2, runs 12, 18–20). The effect of the metal particle size on both the TOF and the selectivity is believed to be brought about by "geometric" and/or "electronic" size effects [3,4,16,18]. Now we discuss how these effects could be manifested and how we can explain the observed changes in the activity and selectivity.

In the ideal case, the shape of nano-sized gold should be a cuboctahedron [19]. Therefore, we use a cuboctahedron geometrical model of the particle (Fig. 2a) suggested by Van Hardefeld and Hartog [18] and the dependence of the ratio of various surface atoms on the particle diameter for the cuboctahedron model (Fig. 2b) calculated by Mohr and Claus [16] to correlate the changes of TOF with the ratio of various types of surface atoms (see Fig. 2b). One can see that as d(Au) decreases, the overall fraction of gold atoms with low coordination number (6 and 7, corner and edge atoms) increases, whereas the fraction of plane atoms with high coordination number (8 and 9) decreases (Fig. 2b). Thus now we can link the increase in the concentration of low-coordinated atoms (Fig. 2b) to the observed increase in TOF in hydrogenation (Table 1, runs 1, 2 and Table 2, runs 12, 18–20). As a result, we can propose that the corner and edge atoms are the most active part of the gold nanoparticle surface.

A study that fully supports the above thesis was carried out by Mohr and Claus [15]. They measured the activity and selectivity of gold nanoparticles, both neat and with indium-decorated faces, in the acrolein hydrogenation. The TOF on 9.0-nm neat gold nanoparticles and 10-nm gold nanoparticles with indium-decorated gold faces were 0.1 and 0.05 s^{-1} respectively [15]. If we take into account that indium was inactive in hydrogenation and that after decoration 100% of gold nanoparticle surface planes and approximately 40–50% of gold nanoparticle edges and corners[1]

[1] Although the authors did not mention that, the decoration of some edges and corners could be easily seen on their Au-In HRTEM images (Fig. 7c).

were isolated from the reaction, the reported results clearly demonstrate that the most active sites for hydrogenation should be exactly the edge and/or corner gold atoms. One more piece of evidence for superior activity of the corner and edge atoms in contrast to the plane atoms was obtained by Bus and Jia. On the basis of careful analysis of Au/Al_2O_3 by *in situ* X-ray absorption spectroscopy, chemisorption, and H/D exchange experiments, Bus and Miller [20] has found that only the corner and edge gold atoms could induce hydrogen dissociation. The elucidated dependences of hydrogen chemisorption and TOF in acetylene hydrogenation on the size of supported metal particles obtained by Jia et al. [7] are similar to the results reported by Bus [9,20]. Now, summarizing the above results we can explain the influence of the "Geometric" effect on the TOF in the hydrogenation of acetylene compounds: as the gold nanoparticle size decreases, the proportion of surface sites responsible for hydrogenation (edges and corners) increases, and this is manifested in the increase in thee hydrogenation rate.

To discuss the role of "Geometric" effect in the dependence of the selectivity on the particle size (Table 2, runs 12, 18–20), first examine the hydrocarbon adsorption on the corners, edges and planes of gold nanoparticles. Outka has studied the adsorption of ethylene and acetylene on Au(1 1 0) crystal plane by TPD [21]. For both hydrocarbons, a single broad desorption peak between 125 and 200 K was observed with no signs of decomposition products. Koel [21] has studied the adsorption properties of cyclohexane and cyclohex-1-ene on Au(1 1 1) crystal plane. These substrates undergo reversible adsorption without decomposition. The binding energies of dec-1-ene, n-decane, hex-1-ene and n-hexane on Au(1 1 1) crystal plane are 81.1, 80.1, 56.6, 56 kJ/mol respectively [22]. So there is no significant difference between adsorption of acetylenes, alkenes or alkanes on gold planes. Differences in the adsorption behavior arise as gold planes are replaced by a combination of gold planes, corners and edges. Jia et al. [7] has shown that the amount of acetylene adsorbed on 3.8-nm gold particles immobilized on Al_2O_3 was 18 times greater than that of ethylene. Moreover, in contrast to ethylene, adsorption of acetylene was irreversible. Segura et al. [8] has demonstrated that 4-nm gold nanoparticles supported on CeO_2 are extremely selective in the hydrogenation of triple bonds in propyne–propene mixtures. His DFT simulations proved that the observed selectivity is related to the stronger adsorption of prop-1-yne compared with propene on edges of supported gold. The results described clarify the role of the "Geometric" effect in the dependence of styrene selectivity on particle size observed by our group (Table 2, runs 12, 18–20) as the high selectivity of small gold nanoclusters in acetylene hydrogenation (Table 1, runs 1, 2). As the particle size decreases, the ratio of (corners + edges) to (planes) increases. This leads to essential increase in the adsorption of acetylene compounds relative to corresponded olefins. This results in an increase in selective hydrogenation of acetylene compounds from alkyne–olefin mixtures.

It is known that electronic properties of metal particles can change appreciably when the number of atoms in an isolated metal particle is reduced. This is so called "electronic" or "ligand" effect. There is much evidence to indicate that very small metal particles do not have the band structure characteristic of bulk metals and they appear to be electron deficient [3]. In other words, as the particle size decreases, the electron deficiency increases. This can have a strong influence on the adsorption behavior by changing (usually increasing) the adsorption energy of unsaturated compounds and increasing the hydrogenation rate [16]. In the supported gold catalysts, some supports can behave as electron acceptors or donors and thus affect the adsorption and hydrogenation rate of unsaturated compounds. Electron transfer from the support to gold was found in Au/TiO_2 systems, resulting in a decrease in the C=C bond hydrogenation rate [4,5,21]. In the case of Au/Al_2O_3 catalysts, the situation is opposite: gold nanoparticles donate electrons to the support [11,21,23,24]. Of course, the chemisorption of electron-rich substrates such as alkynes on these more electron-deficient gold particles should be more preferable. The latter should lead to increasing of TOF and selectivity. Thus, the "Electronic" size effect can explain the increase in the TOF and selectivity of acetylene hydrogenation from alkyne-olefin mixtures observed in this work (Table 1, runs 1, 2 T = 370–390 K and Table 2, runs 12, 18–20).

4. Conclusions

2.5–30 nm gold nanoparticles possess high activity, selectivity and stability in hydrogenation of acetylene and phenylacetylene into the corresponding olefin from alkyne-olefin mixture at 360–423 K. An increase in the TOF and selectivity by an order of magnitude for smaller gold particles was found. This trend can be attributed to the increased surface concentration of corner and edge gold atoms in small particles and/or to increased electron deficiency and positive surface charge of small particles supported on Al_2O_3.

$Au\text{-}Ni/Al_2O_3$ nanocomposites demonstrate higher activity and stability in hydrogenation of acetylene into ethylene from acetylene–ethylene mixture in comparison with mono- and bimetallic catalysts based on Pd, Ag and Ni. A strong synergistic effect of the activity was revealed for Au-Ni catalysts: the conversion of acetylene on the Au-Ni catalysts was higher than the sum of conversions on Au and Ni catalysts. Reasons for the synergistic behavior are discussed in terms of formation of new $A^{\sigma+}$ catalytic sites due to electron transfer from electron-rich gold to electron-deficient nickel.

Acknowledgements

This work was supported by the RFBR (grant no. 08-03-00389) and Federal agency on a science and innovations (project no. 02.513.11.3466). S.A. Nikolaev was also supported by the Council of President grants for the young scientists (grant MK-5703.2008.3).

References

[1] A. Borodziński, G.C. Bond, Catal. Rev. Sci. Eng. 48 (2006) 91.
[2] James T. Merrill, Pat. US 7,105,711 B2, Fina Technology Ink (2006).
[3] A. Molnar, A. Sarkany, M. Varga, J. Mol. Catal. A: Chem. 173 (2001) 185.
[4] G.C. Bond, D.T. Thompson, Catal. Rev. Sci. Eng. 41 (1999) 319.
[5] A. Hashmi, K. Stephen, G.J. Hutchings, Angew. Chem. Int. Ed. 45 (2006) 7896.
[6] J.A. Lopez-Sanchez, D. Lennon, Appl. Catal. A: Gen. 291 (2005) 230.
[7] J. Jia, K. Haraki, J.N. Kondo, K. Domen, K. Tamaru, J. Phys. Chem. B 104 (2000) 11153.
[8] Y. Segura, N. López, J. Pérez-Ramírez, J. Catal. 247 (2007) 383.
[9] E. Bus, R. Prins, J.A. van Bokhoven, Catal. Commun. 8 (2007) 1397.
[10] V.V. Smirnov, S.A. Nikolaev, G.P. Murav'eva, L.A. Tyurina, A. Yu. Vasil'kov, Kinet. Catal. 48 (2007) 265 [Engl. Transl.].
[11] O.P. Tkachenko, L.M. Kustov, S.A. Nikolaev, V.V. Smirnov, K.V. Klementiev, A.V. Naumkin, I.O. Volkov, A.Yu. Vasil'kov, D. Yu, Murzine Top. Catal. 52 (2009) 344.
[12] F. Besenbacher, I. Chorkendorff, B.S. Clausen, B. Hammer, A.M. Molenbroek, J.K. Nørskov, I. Stensgaard, Science 279 (1998) 1913.
[13] M. Okumura, T. Akita, M. Haruta, Catal. Today 74 (2002) 265.
[14] C. Mohr, H. Hofmeister, P. Claus, J. Catal. 213 (2003) 86.
[15] C. Mohr, H. Hofmeister, J. Radnik, P. Claus, J. Am. Chem. Soc. 125 (2003) 1905.
[16] C. Mohr, P. Claus, Sci. Prog. 84 (2001) 311.
[17] T.V. Choudhary, C. Sivadinarayana, A.K. Datye, D. Kumar, D.W. Goodman, Catal. Lett. 86 (2003) 1.
[18] R. Van Hardeveld, F. Hartog, Surf. Sci. 15 (1969) 189.
[19] C.R. Henry, Surf. Sci. Rep. 31 (1998) P.235.
[20] E. Bus, J.T. Miller, J.A. van Bokhoven, J. Phys. Chem. B 109 (2005) 14581.
[21] R. Meyer, C. Lemire, Sh.K. Shaikhutdinov, H.-J. Freund, Gold Bull. 37 (2004) 72.
[22] R.J. Baxter, G. Teobaldi, F. Zerbetto, Langmuir 9 (2003) 7335.
[23] C.K. Costello, J.H. Yang, H.Y. Law, Y. Wang, J.N. Lin, L.D. Marks, M.C. Kung, H.H. Kung, Appl. Catal. A: Gen. 243 (2003) 15.
[24] H.H. Kung, M.C. Kung, C.K. Costello, J. Catal. 216 (2003) 425.